

## Neutron angular distribution in $(\gamma, n)$ reactions with linearly polarized $\gamma$ -ray beam generated by laser Compton scattering



K. Horikawa<sup>a</sup>, S. Miyamoto<sup>a</sup>, T. Mochizuki<sup>a</sup>, S. Amano<sup>a</sup>, D. Li<sup>b</sup>, K. Imasaki<sup>b</sup>, Y. Izawa<sup>b</sup>,  
K. Ogata<sup>c</sup>, S. Chiba<sup>d,e</sup>, T. Hayakawa<sup>e,f,\*</sup>

<sup>a</sup> University of Hyogo, Hyogo 678-1205, Japan

<sup>b</sup> Institute for Laser Technology, 2-6 Yamada-oka, Suita, Osaka 565-0871, Japan

<sup>c</sup> Osaka University, 1-1 Yamadaoka, Suita, Osaka 565-0871, Japan

<sup>d</sup> Tokyo Institute of Technology, 2-12-1 Ookayama, Meguro-ku, Tokyo 152-8550, Japan

<sup>e</sup> Japan Atomic Energy Agency, Shirakata-Shirane 2-4, Tokai-mura, Ibaraki 319-1195, Japan

<sup>f</sup> National Astronomical Observatory, Mitaka, Tokyo 181-8588, Japan

### ARTICLE INFO

#### Article history:

Received 9 October 2013

Received in revised form 11 August 2014

Accepted 12 August 2014

Available online 15 August 2014

Editor: V. Metag

#### Keywords:

Linear polarized  $\gamma$ -ray

Photodisintegration reactions

M1 strength

Giant dipole resonance

Neutron angular distribution

### ABSTRACT

In 1957, Agodi predicted that the neutron angular distribution in  $(\gamma, n)$  reactions with a 100% linearly polarized  $\gamma$ -ray beam for dipole excitation should be anisotropic and universally described by the simple function of  $a + b \cdot \cos(2\phi)$  at the polar angle  $\theta = 90^\circ$ , where  $\phi$  is the azimuthal angle. However, this prediction has not been experimentally confirmed in over half a century. We have verified experimentally this angular distribution in the  $(\gamma, n)$  reaction for  $^{197}\text{Au}$ ,  $^{127}\text{I}$ , and natural Cu targets using linearly polarized laser Compton scattering  $\gamma$ -rays. The result suggests that the  $(\vec{\gamma}, n)$  reaction is a novel tool to study nuclear physics in the giant dipole resonance region.

© 2014 The Authors. Published by Elsevier B.V. This is an open access article under the CC BY license (<http://creativecommons.org/licenses/by/3.0/>). Funded by SCOAP<sup>3</sup>.

Photonuclear reactions have an important role for developing nuclear physics [1] and for various applications such as non-destructive measurements of nuclear materials [2,3]. Recent progress in accelerator and laser physics has led to a new generation of photon beams, based on the technique of laser Compton scattering (LCS). Energy tunable quasi-monochromatic LCS  $\gamma$ -ray beams in the MeV energy region have been used for fundamental science and various applications at Duke University [4], the National Institute of Advanced Industrial Science and Technology in Japan [5], and NewSUBARU in Japan [6]. An advantage of the LCS  $\gamma$ -ray beams comes from the fact that one can generate almost 100% linearly (circularly) polarized beams since the polarization of the laser is directly transferred to the scattered photons.

The polarized  $\gamma$ -rays have been widely used for the study of the nuclear structure via nuclear resonance fluorescence (NRF). With linearly polarized photons, the parity of each excited state in a nucleus is obtained by measuring the angular distribution of the emitted  $\gamma$ -ray yields. As a result, electric-dipole (E1) and

magnetic-dipole (M1) transition strengths from the ground state can be measured directly (for examples, see Refs. [7,8]). In the photon energy region above the neutron threshold, the  $(\gamma, n)$  reaction is the dominant process in most nuclei and has been studied using non-polarized  $\gamma$ -rays (for example, Refs. [9,10].) Thus, the  $(\gamma, n)$  reaction with linearly polarized  $\gamma$ -ray beams has the potential to be used for studying detailed nuclear structures as NRF.

One important topic in the energy region above the neutron threshold is M1 strength. The “missing” M1 strength still remains an unsolved problem in nuclear physics [1]. A part of the missing M1 strength may be in the giant dipole resonance (GDR) region. The M1 strength is often used to estimate the interaction strength between neutrinos and nuclei in astrophysics. The neutrino-nucleus interaction plays an extremely important role for supernova explosions and syntheses of several rare isotopes [11–13]. However, there is no effective method to measure the M1 strength in the GDR region because of the overlap between the weak M1 strength and the strong E1 strength, although techniques like proton inelastic scattering [14] and total photodisintegration cross-section measurements [15] have been developed.

In the 1950s, angular distribution of cross sections for  $(\vec{\gamma}, n)$  and  $(\vec{\gamma}, p)$  reactions were calculated [16,17]. Agodi [17] predicted,

\* Corresponding author.

E-mail address: hayakawa.takehito@jaea.go.jp (T. Hayakawa).



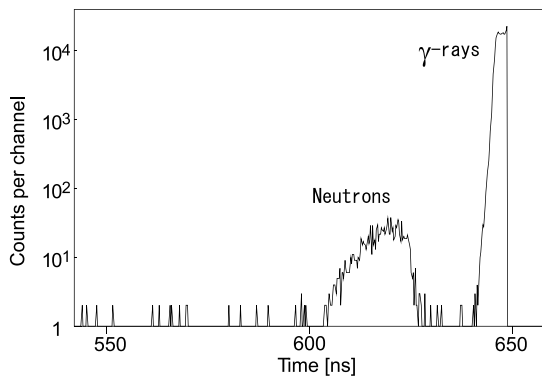


**Fig. 2.** Time-of-flight spectrum on the  $^{197}\text{Au}(\text{polarized } \gamma, n)^{196}\text{Au}$  reaction at  $\phi = 90^\circ$ . The peaks of prompt  $\gamma$ -rays and neutrons are clearly separated. Natural background by radioactivity and cosmic rays are much lower than these signals.

the laser beam was extracted to the outside of the electron storage ring after the  $\gamma$ -ray generation without additional mirrors and the polarization angle was measured by a combination of a laser power meter and a Glan–Thompson prism. The polarization angle was determined by changing the angle of the Glan–Thompson prism until the angle was found which maximized the transmitted laser power. We measured the neutron energy spectra as a function of the laser polarization angle in a range from  $\phi = 0^\circ$  to  $360^\circ$  in  $30^\circ$  steps for NaI and Cu, where the  $\phi = 0^\circ$  was defined as the electric polarization vector being in the plane of the detector. We measured only 9 angles for the Au measurement to obtain high statistics.

**Fig. 2** shows a TOF spectrum from the  $^{197}\text{Au}$  measurement. The neutrons and prompt  $\gamma$ -rays are clearly separated. The energy spectra of the neutrons were derived from the TOF signals. Neutrons with energies lower than 2 MeV were not measured because of the detection efficiency. The measured maximum energy of the neutrons is about 8 MeV for Au. This energy is consistent with an expected energy of 8.6 MeV, the difference between the maximum photon energy of 16.7 MeV and the neutron separation energy of 8.1 MeV (see **Fig. 1**).

One of the excellent features of the LCS  $\gamma$ -ray beam is its short pulse length. The duration of the generated LCS  $\gamma$ -ray pulse is equal to the width of the shorter pulse of the electron and laser in the case of “head-on collision.” The widths of the laser and the electron were 8 ns and 60 ps, respectively. Thus, the pulse width of the LCS  $\gamma$ -ray beam should be only 60 ps. The measured time width of the prompt  $\gamma$ -rays is, however, about 3 ns because of time fluctuation of the slow rise-time photomultiplier and the time jitter between the laser generation time and the external trigger signal from the electron storage ring. On the other hand, the time resolution, originating from the ratio of the detector thickness to the flight path length, was about 5%. Furthermore, the final energy resolution in the present setup was determined by the energy spread of the incident beam, since the incident beam energy spread of 3–5 MeV were wider than the energy resolution of about 5%, for example about 0.4 MeV at 8 MeV. These energy spreads of 3–5 MeV are much wider than the energy level spacing in the target nuclei. Thus, the level structures of the residual nuclei cannot be observed in the TOF spectra.

**Fig. 3** shows the angular distributions of the  $(\bar{\gamma}, n)$  reactions for the three targets. The neutron yields are presented as a function of the azimuthal angle  $\phi$ . The solid lines show the function of  $a + b \cdot \cos(2\phi)$  obtained by  $\chi^2$ -fitting. The natural Cu consists of two stable isotopes  $^{63}\text{Cu}$  (69%) and  $^{65}\text{Cu}$  (31%). The sum for the two isotopes is also reproduced by this function. The NaI target consists of  $^{23}\text{Na}$  and  $^{127}\text{I}$ . Since the neutron separation energies of these nuclides are 12.4 MeV ( $^{23}\text{Na}$ ) and 9.1 MeV ( $^{127}\text{I}$ ) the contribution

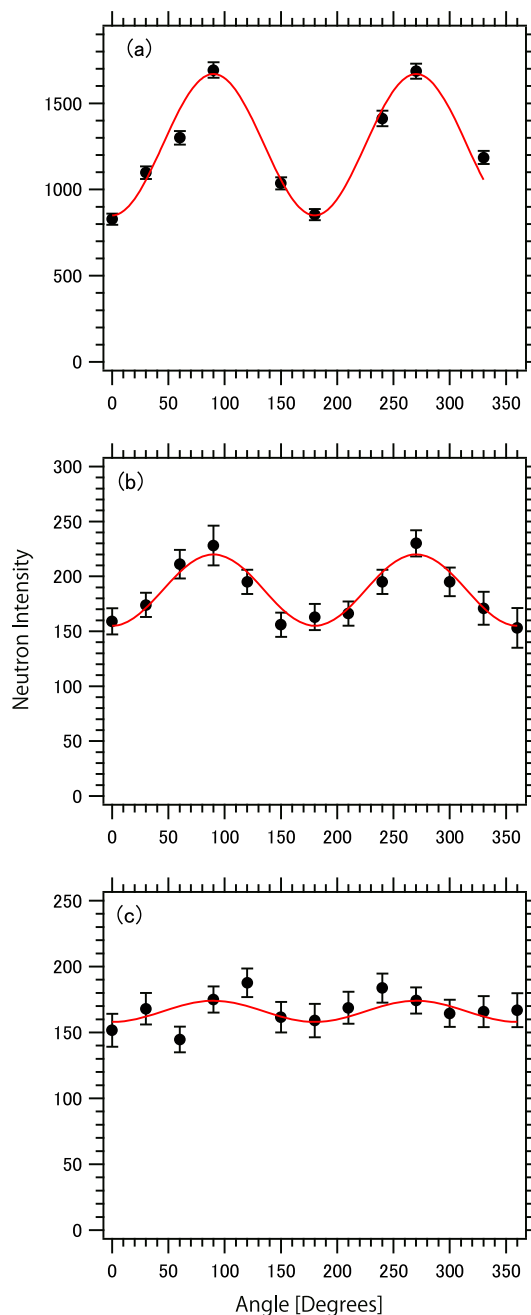


**Fig. 3.** Angular distributions of neutrons of  $(\bar{\gamma}, n)$  reactions on (a) Au, (b) NaI, and (c) natural Cu targets. The solid lines are obtained by  $\chi^2$ -fitting with a function of  $a + b \cdot \cos(2\phi)$  predicted by Agodi in 1957. This function reproduces well these three data and thereby this prediction is experimentally examined for the first time over the wide range.

of  $^{127}\text{I}$  is dominant for the NaI target. We would like to stress that the three neutron angular distributions are well described as the function of  $a + b \cdot \cos(2\phi)$  independent of nuclides. Therefore, the theoretical prediction by Agodi is for the first time verified over the wide mass region.

A question we have to address here is why the anisotropy,  $b/a$ , increases with increasing atomic number of the targets. The GDR peak energy decreases, in general, with increasing atomic number. The level density in heavy nuclei is relatively high and the wave function becomes more complex. There are many types of transitions of which the sign of the parameter  $b$  are different from each other. As a result, the anisotropy of the neutron angular distribu-

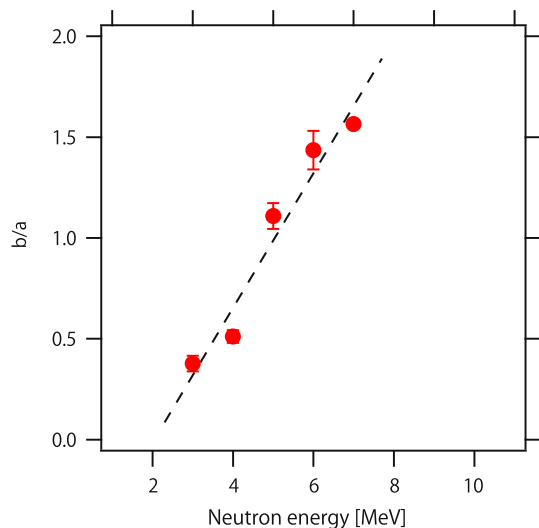


**Fig. 4.** Plot of the anisotropy,  $b/a$ , of the neutron angular distribution as a function of neutron energy for  $^{197}\text{Au}$ . The dashed line is a guideline. The anisotropy increases with increasing the neutron energy. This can be explained by the number of the transitions (see the main text).

tion in heavy nuclei is expected to decrease. However, the present result is opposite to this expectation.

For a more detailed investigation of the relatively strong anisotropy measured in the  $^{197}\text{Au}(\gamma, n)^{196}\text{Au}$  reaction, we plot the anisotropy,  $b/a$ , as a function of the neutron energy in Fig. 4. It is clearly shown that the  $b/a$  ratio increases with increasing neutron energy. We also evaluate  $b/a$  values for NaI and Cu. The NaI anisotropy is  $0.77 \pm 0.08$  ( $0.17 \pm 0.09$ ) for 4–8 MeV (2–4 MeV). The Cu anisotropy is  $0.30 \pm 0.09$  ( $-0.05 \pm 0.07$ ) for 4–7 MeV (2–4 MeV). In the cases of NaI and Cu, the anisotropy also increases with increasing neutron energy. These three results lead to the conclusion that the anisotropy for all transitions as shown in Fig. 4 originates from the contribution of the high energy neutrons.

The trend that the anisotropy increases with increasing neutron energy can be understood by taking into account the number of combinations of an initial state before neutron emission and a final state. Since the incident  $\gamma$ -ray beam has an energy spread of about 5 MeV for Au, many excited states in  $^{197}\text{Au}$  with an energy range of 12–17 MeV are populated. High energy neutrons decay from highly excited states near the maximum energy 17 MeV in  $^{197}\text{Au}$  to the ground state or a low excited state on the residual nucleus  $^{196}\text{Au}$  (see the solid arrows in Fig. 1). Thus, the anisotropy of these specific transitions can be selectively observed with the gate on high neutron energy. In contrast, in the case of the low energy neutron gate, there are a large number of transitions (see the dashed arrows in Fig. 1). The angular distribution of the low energy neutrons is the summation of these multiple transitions. The sign of a part of the transitions should be opposite to that of the other and thus the anisotropy of the summation decreases.

The maximum energy of the incident LCS beam was fixed to 16.7 MeV, whereas the neutron separation energy decreases with increasing the atomic number ( $^{197}\text{Au}$ : 8.1 MeV,  $^{127}\text{I}$ : 9.1 MeV,  $^{63}\text{Cu}$ : 10 MeV,  $^{65}\text{Cu}$ : 9.9 MeV). Thus the energy difference increases with increasing the atomic number. This suggests that the percentage of high energy neutrons is high in heavy nuclei. Thus, the result that the strongest anisotropy is observed for the heaviest nucleus,  $^{197}\text{Au}$ , can be understood in terms of the neutron separation energy.

The anisotropy for all the transitions originates from the contribution of the high energy neutrons as discussed above. This indicates that the M1/E1 mixing in heavy nuclei can be evalu-

ated from a polarization asymmetry at  $\theta = 90^\circ$  (or other angles) by gating with the highest neutron energy to select the transition to the ground state of the residual nucleus as the previous studies using  $(\vec{\gamma}, p)$  reactions [19,20]. Ogata et al. show that the parameters,  $a$  and  $b$ , depend on the charge transition density for both  $(\vec{\gamma}, n)$  and  $(\vec{\gamma}, p)$  reactions [29]. With theoretical calculations for the charged transition density, we can study the detailed nuclear structure in the GDR region.

For such a purpose, the key point is the energy resolution of neutron measurements. In the present experiment, the energy resolution is finally determined by the energy width of the incident  $\gamma$ -ray beam. The typical energy spread of the photon beam is 3–10% in the present available LCS  $\gamma$ -ray facilities. With 17-MeV  $\gamma$ -rays, the neutron energy resolution is about 0.5–1.7 MeV. This suggests that we should select a target nucleus in which the energy of the first excited state is higher than 0.5 MeV (if the energy spread of the incident beam is 3%) or that we should measure the summation of some transitions to the ground state and low excited states. The progress in laser and accelerator physics enables us to realize the next generation of the LCS  $\gamma$ -ray sources including ELLNP [30], MEGA-ray [31], and the ERL-LCS [32]. The extended plan of the HI $\gamma$ S can be included in them [33]. The energy spread of these  $\gamma$ -ray beams is expected to be lower than  $dE/E \sim 10^{-3}$ . If we couple the present experimental method with a high energy resolution  $\gamma$ -beam, it is possible to study the detailed nuclear structure of the GDR with an excellent resolving power of the order of keV.

Finally we would like to point out that the present method is applicable in the energy region above the 2 neutron separation energy. Even when  $(\gamma, xn)$  ( $x \geq 2$ ) reaction channels open, the  $(\gamma, n)$  channel is also still open and we can selectively measure the  $1n$  reaction channel by gating the maximum neutron energy, which corresponds to the transition from excited states near the highest populated level to the ground state of the residual nucleus.

In summary, we measured the neutron angular distribution at the polar angle  $\theta = 90^\circ$  from  $(\gamma, n)$  reactions on three targets of Au, NaI, and Cu with a linearly polarized laser Compton scattering  $\gamma$ -ray beam at NewSUBARU. In 1957, Agodi predicted that angular distributions in  $(\gamma, n)$  and  $(\gamma, p)$  reactions with a 100% linearly polarized  $\gamma$ -ray beam should be anisotropic and described as a simple function of  $a + b \cdot \cos(2\phi)$  at  $\theta = 90^\circ$  from the conservation laws of angular momentum and parity. However, this prediction has not been experimentally confirmed in over half a century. The anisotropy may vanish in heavy nuclei because of their complex nuclear structures. However, the present experimental result clearly shows that the angular distributions are well described by the function  $a + b \cdot \cos(2\phi)$  for the three nuclei. In addition, we found that the anisotropy originated from high energy neutrons, corresponding to the transition from highly excited levels to the ground state or a low excited state in the residual nucleus. In the near future, the next generation of the LCS  $\gamma$ -rays will be available. The lost Agodi's prediction will have a more precious role to study nuclear physics in the GDR region and applications using photonuclear reactions.

## Acknowledgements

This work has been supported in part by Grants-in-Aid for Scientific Research (25610061, 24340060, 22740169, 23654204) of the Japan Society for the Promotion of Science.

## References

- [1] K. Heyde, et al., *Rev. Mod. Phys.* **82** (2010) 2365.
- [2] J.L. Jones, et al., *Nucl. Instrum. Methods Phys. Res., Sect. B, Beam Interact. Mater. Atoms* **241** (2005) 770.

- [3] T. Hayakawa, et al., Nucl. Instrum. Methods Phys. Res., Sect. A, Accel. Spectrom. Detect. Assoc. Equip. 621 (2010) 659.
- [4] V.N. Litvinenko, et al., Phys. Rev. Lett. 78 (1997) 4569.
- [5] H. Ohgaki, S. Sugiyama, T. Yamazaki, T. Mikado, M. Chiwaki, K. Yamada, R. Suzuki, T. Noguchi, T. Tomimasu, IEEE Trans. Nucl. Sci. 38 (1991) 386.
- [6] S. Miyamoto, et al., Radiat. Meas. 41 (2007) S179.
- [7] N. Pietralla, et al., Phys. Rev. Lett. 88 (2001) 012502.
- [8] T. Shizuma, et al., Phys. Rev. C 78 (2008) 061303(R).
- [9] M. Rahman, et al., Nucl. Instrum. Methods Phys. Res., Sect. B, Beam Interact. Mater. Atoms 268 (2010) 13.
- [10] C. Plasisir, et al., Eur. Phys. J. A 48 (2012) 68.
- [11] S.E. Woosley, Astrophys. J. 356 (1990) 272–301.
- [12] A. Byelikov, et al., Phys. Rev. Lett. 98 (2007) 082501.
- [13] T. Hayakawa, T. Kajino, S. Chiba, G.J. Mathews, Phys. Rev. C 81 (2010) 052801(R).
- [14] A. Tamii, et al., Phys. Rev. Lett. 107 (2011) 062502.
- [15] H. Utsunomiya, et al., Phys. Rev. Lett. 100 (2008) 162502.
- [16] G.R. Satchler, Proc. Phys. Soc. 68A (1955) 1041.
- [17] A. Agodi, Nuovo Cimento 5 (1) (1957) 21.
- [18] E.M. Kellogg, W.E. Stephens, Phys. Rev. 149 (1966) 798.
- [19] K. Wienhard, et al., Phys. Rev. C 24 (1981) 1363.
- [20] A. de Rosa, et al., Nuovo Cimento 40 (1984) 401.
- [21] A. De Shalit, H. Feshbach, Theoretical Nuclear Physics: Nuclear Structure, John Wiley & Sons Inc., 1974.
- [22] M.W. Ahmed, et al., Phys. Rev. C 77 (2008) 044005.
- [23] M.A. Blackston, et al., Phys. Rev. C 78 (2008) 034003.
- [24] W.F. Lawrence, S.S. Stanley, Rev. Mod. Phys. 31 (1959) 711.
- [25] R. Raphael, H. Uberall, Nucl. Phys. 85 (1966) 327.
- [26] T. Hayakawa, et al., Phys. Rev. C 74 (2006) 065802.
- [27] T. Hayakawa, et al., Phys. Rev. C 77 (2008) 068801.
- [28] K. Horikawa, S. Miyamoto, S. Amano, T. Mochizuki, Nucl. Instrum. Methods Phys. Res., Sect. A, Accel. Spectrom. Detect. Assoc. Equip. 618 (2010) 209.
- [29] K. Ogata, T. Hayakawa, S. Chiba, 2013, in preparation.
- [30] D. Habs, T. Tajima, V. Zamfir, Nucl. Phys. News 21 (2011) 23.
- [31] F. Albert, et al., Phys. Rev. Spec. Top., Accel. Beams 14 (2011) 050703.
- [32] R. Hajima, T. Hayakawa, N. Kikuzawa, E. Minehara, J. Nucl. Sci. Technol. 45 (2008) 441.
- [33] <http://www.tunl.duke.edu/higs2.php>.